Ultralight Deployable Space Structure Prototype

Eleftherios E. Gdoutos,* Alan Truong,† Antonio Pedivellano,‡ Fabien Royer,§ and Sergio Pellegrino¶
California Institute of Technology, Pasadena, CA, 91125

We present a lab demonstration of the packaging and deployment of an ultralight space structure prototype composed of thin shell longerons and battens. The prototype is integrated with a thin polyimide membrane which serves as mass representative of multi-functional elements that could be integrated into this type of deployable, such as integrated power collection and wireless transmission tiles for space solar power. A deployment mechanism using actively controlled pressure to package and deploy this structure ensuring its integrity is described. The deployable structure and deployment mechanism designs are scalable to 60 m $\times$ 60 m structures. The structure's mass scaling to larger sizes is described.

I. Introduction

Tightly packageable, ultralight, and bending-stiff deployable structures have been previously proposed for space solar power [1] and other high performance applications [2, 3]. Figure 1a shows such a conceptual space structure. The structure is composed of independent bending-stiff trapezoid strips that are held together by four diagonal cords. The packaging and deployment concept is shown in Figure 1b [2].

This type of structure structure could deploy packageable multi-functional elements that collect sunlight, convert it to RF electrical power, and wirelessly transmit that power through a phased array to a distant receiver [4–6]. In 2019, the Caltech team demonstrated the first lab prototype of an ultralight (150 g/m^2), bending-stiff space structure scalable to 60 $\times$ 60 m and designed for integration with multi-functional elements [7].

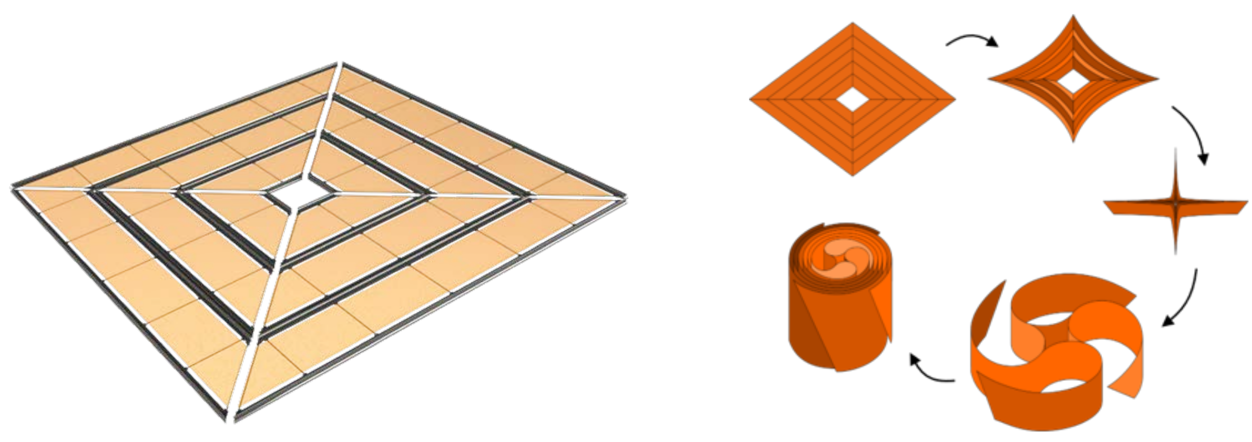

(a) (b)

Fig. 1 (a) Deployable structure concept consisting of thin shell longerons and battens; and (b) packaging concept.

Here, we present the packaging and deployment of a prototype ultralight space structure composed of thin-shell longeron bending-stiff trapezoid strips integrated with a functional element surrogate. Thin shell longeron design, manufacture, and assembly into a structure were critical to enable the structure's coiling and deployment. The coiling

*Research Scientist, Graduate Aerospace Laboratories, MC 105-50. AIAA Member. E-mail: egdoutos@caltech.edu.
†Research Engineer, Graduate Aerospace Laboratories, MC 105-50.
‡Graduate Student, Graduate Aerospace Laboratories, MC 105-50. AIAA Student Member.
§Graduate Student, Graduate Aerospace Laboratories, MC 105-50. AIAA Student Member.
¶Joyce and Kent Kresa Professor of Aerospace and Civil Engineering; Jet Propulsion Laboratory Senior Research Scientist; Co-Director, Space-Based Solar Power Project, Graduate Aerospace Laboratories, MC 105-50. AIAA Fellow. E-mail: sergiop@caltech.edu.

and folding characteristics of the structure were studied and a scalable deployment mechanism applying external pressure to package and deploy the structure was designed and assembled.

The prototype components are designed for the bending stiffness of a structure up to 60 m x 60 m. However, for lab demonstration, the longest component is 1.7 m. This prototype demonstrates the deployment of an ultralight tightly packaged structure of thin shell longerons and battens designed with structural and mechanical properties for a spacecraft enabling space solar power and other high performance applications.

II. Prototype description

We have designed, built, and tested a 1677 mm × 1677 mm deployable space structure prototype composed of 12 trapezoid strips (Figure 2). The prototype design parameters and overall size were the same as in the prototype described previously by the Caltech team [7]. The strips consist of thin shell TRAC [8] cross section longerons and rectangular cross section battens. Strips are geometrically defined by the length of their longest longeron, the strip width, and the batten spacing. Strip width (0.2 m) and batten spacing (0.3 m) were the same as in the previous prototype. The 12 strips are assembled into a structure by connecting to four cords, each running between the center and a corner of the structure. Strip spacing and quadrant spacing define how closely the strips are assembled in the full structure. In this prototype the strip spacing was reduced from 10 mm to 6 mm in order to minimize gaps. The quadrant spacing was maintained at 10 mm.

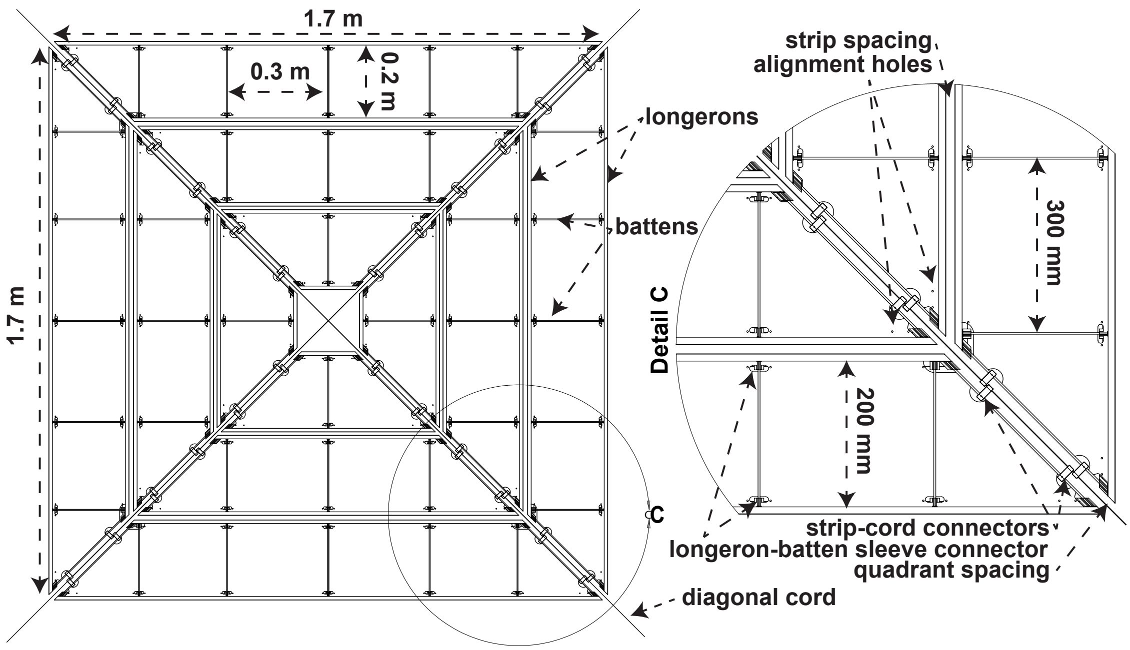

Fig. 2 Drawing of the deployable space structure prototype.

Key differences between the previous prototype and the one described here are deployability and integration with a patterned 50 μm thick polyimide film with areal density approximating multi-functional elements. Repeated longeron coiling and uncoiloing without damage is crucial to the prototype's deployment. Previous longeron characterization and investigation into longeron stress concentration and resulting damage during coiling [9, 10] provided key insight to the design used in this prototype. The longerons are ultra-thin (70 μm per flange, 140 μm in total), lightweight (linear density 7.5 g/m) composite [+-45GF/0CF/+-45GF] laminates manufactured in an autoclave. The longeron web length is 8 mm, the flange radius is 12.4 mm and the average opening angle is 97° [11]. The bending stiffness of these longerons is 10.6 Nm^2 and they can be coiled on a 25 mm diameter hub [11]. The battens are 3 mm × 0.6 mm pultruded CFRP rods, slightly thinner than the battens in our previous prototype (0.8 mm). Longeron-batten connectors with an Ω cross-section made of a 2-ply glass fiber [+-45/+-45] laminate provide a sleeve-like bonding interface between the longerons and the battens. Strip-cord connectors bonded to each strip's diagonal battens to connect the trapezoid strips to the four cords were redesigned to a shape conforming to the structure's coiling scheme based on previous work [12].

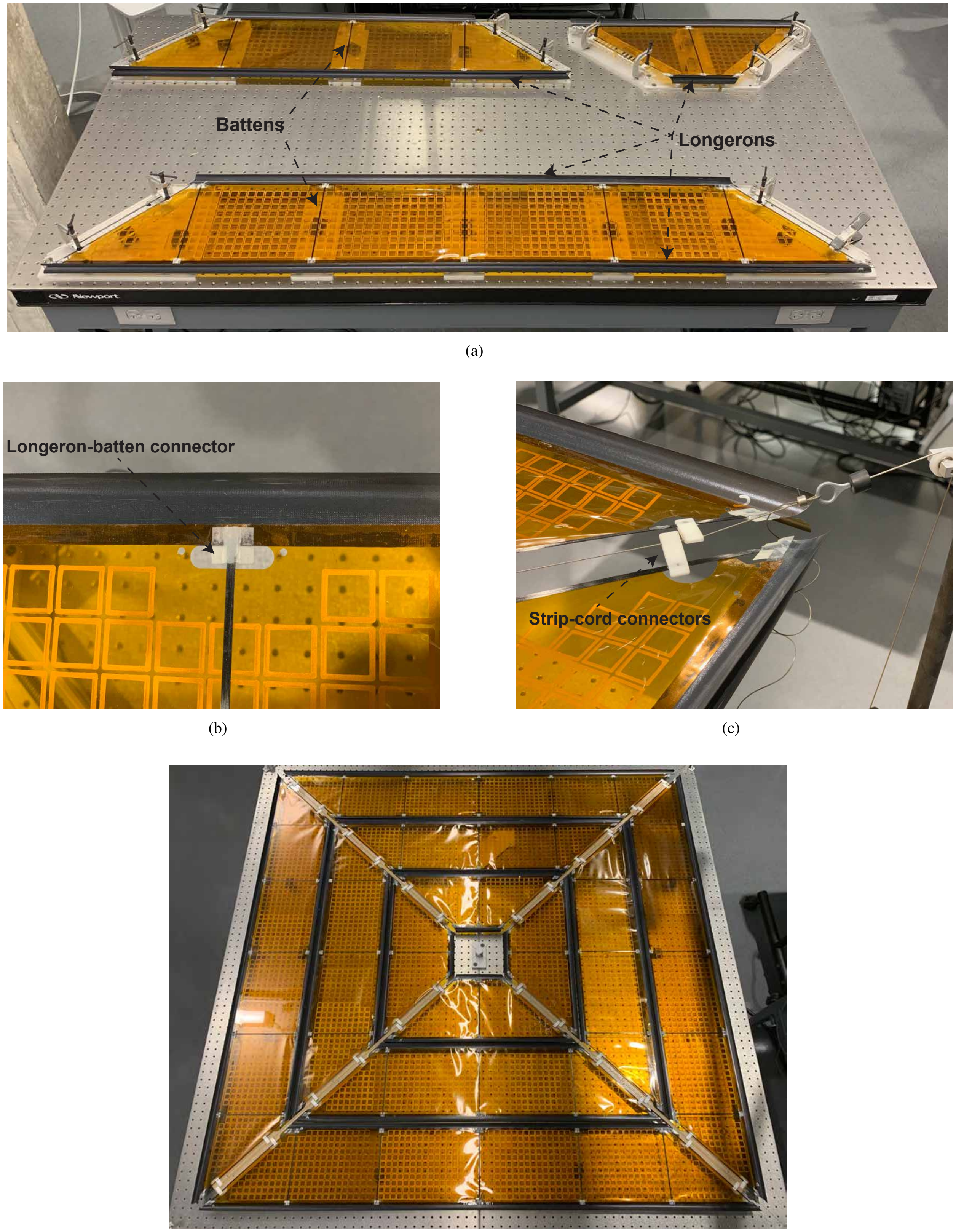

Fig. 3 (a) Three strips composed of thin shell longerons and battens during assembly process; (b) longeron-batten connector joining the longeron to a batten; (c) strip-cord connectors joining two adjacent strips to one of four diagonal cords in the deployable prototype; and (d) deployable prototype assembled on optical table.

A. Strip and prototype assembly

For each strip, a two-step assembly process is adopted to accurately position the prototype's polyimide membrane with respect to the strip-cord connectors and the cords. The membrane is first cut to size with pinhole features to locate it accurately during assembly. The assembly structure is composed of acrylic plates mounted on an optical table. Locating features and pins on the acrylic plates position the polyimide membrane, battens, and longeron-batten connectors within a tolerance of 0.5 mm.

The first step of the strip assembly starts by positioning the polyimide film onto the acrylic plates using the locator pins. The two ends of the battens (Figure 3a) are bonded into the longeron-batten connectors (Figure 3b) and the battens are bonded onto the polyimide. Strip-cord connectors (Figure 3c) are then bonded on the diagonal battens. Clamps are used to apply pressure during bonding. Once the epoxy has fully cured the result is a polyimide membrane bonded to battens, longeron-batten connectors, and strip-cord connectors. The second step of assembly consists of bonding the longeorons into the longeron-batten connectors, and the edge of the polyimide membrane onto the longeron webs. The longerons, positioned by alignment pins, are slid into the longeron-batten connectors and bonded. The design of the longeron-batten connectors allows for manufacturing deviations in the longeron shape. The two longitudinal edges of the polyimide membrane are bonded onto the longeron webs and and clamps are used to apply pressure during bonding.

Three exemplary strips during assembly are shown in Figure 3a. This process is repeated four times, resulting in 12 total strips. An acrylic assembly jig similar to one used for the individual assembly of strips is used to connect the 12 strips to four diagonal cords, completing the prototype. Two acrylic plates per strip (24 total) with features locating the strip-cord connectors within tolerance of 0.5 mm are positioned on the optical table. The strips are then positioned on these acrylic plates. Each strip-cord connector has a slotted hole in which the cord passes through. The four diagonal cords feature a ⌀3.18 mm spherical terminal on one end which is used to connect the cords to the center of the optical tables. Pulleys are positioned at the four corners of the optical table and after passing the cords through the slotted holes of the structure's strip-cord connectors, the cords are tensioned with 0.4 kg weights through the pulleys for the final bonding step of the assembly. The final step of the assembly consists of bonding the cords and the strip-cord connectors. After the epoxy is cured the prototype is completed (Figure 3d). Since the prototype architecture uses bending stiff elements it does not require cord tensioning for stiffness. Two diagonally opposed connectors are bonded to the cord for each strip and the remaining two are left unbonded with the cord free to translate and rotate in the slotted hole. This boundary condition scheme is chosen so that changes in cord tension after assembly do not result in stress on the strips.

B. Packaging concept

The packaging concept for the structure consists of two different stages: folding (Figure 4) and coiling (Figure 5). In the first stage, the strips in each of the four quadrants are folded. Due to the four-fold symmetry of the structure, this process also requires the strips to be folded in the middle by 90 °resulting in a star-like configuration at the end of folding (Figure 4). In the second stage of the packaging, the 4 arms of the star-shape are coiled in a cylindrical configuration, reaching the packaged state. During deployment, the reverse sequence is followed: the structure is first uncoiled from the cylindrical packaged state to the star-shape, and then it is unfolded to the fully-deployed planar configuration.

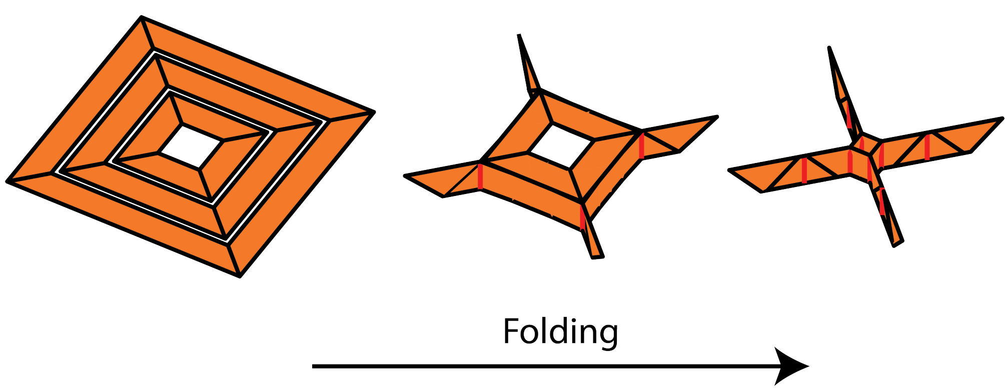

Fig. 4 Folding sequence for the space structure; the red lines correspond to the external constraints, which hold together adjacent strips in the star-shape.

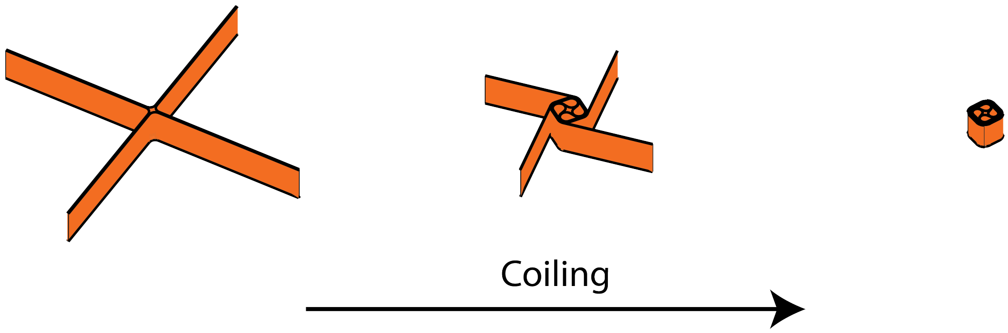

Fig. 5 Coiling sequence for the space structure.

III. Deployment mechanism

A deployment mechanism was developed to test packaging and deployment of the structure. The deployment mechanism, shown in Figure 6 consists of three subsystems: coiling mechanism, cord management system, unfolding constraints. The conceptual design and implementation of each of the subsystems is discussed in detail in the following sections.

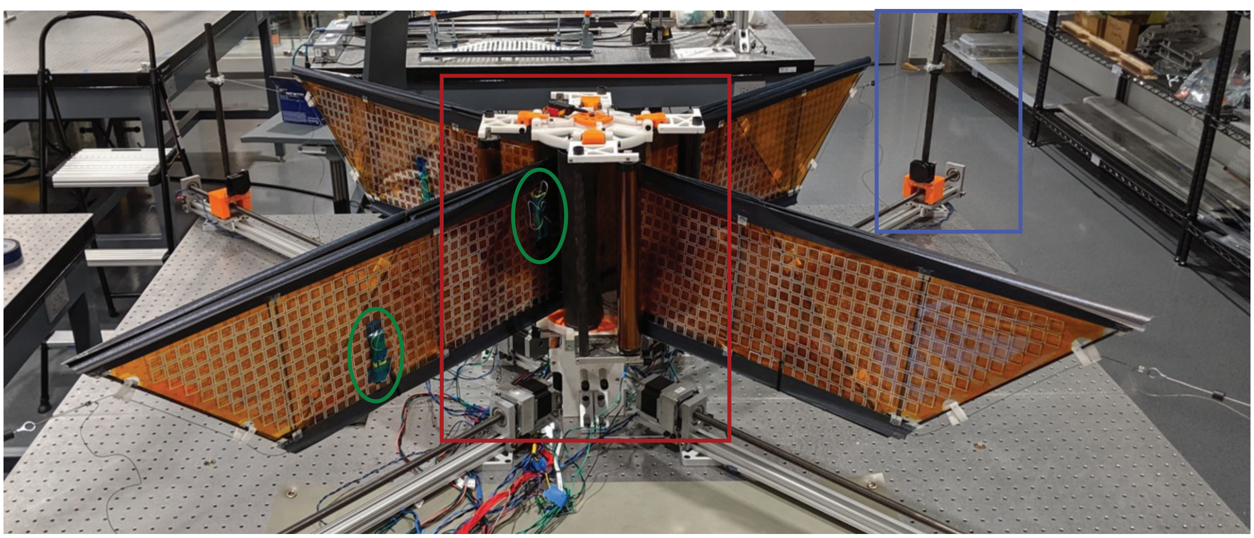

Fig. 6 Deployment mechanism prototype: the coiling mechanism (red box) actively controls and stabilizes the coiling and uncoiling process of the deployable structure; the cord management system (blue box) retracts the diagonal cords during deployment; manually or automatically releasable folding constraints (green circles) locally constrain the strips

A. Coiling

It has been previously observed that structural instabilities such as buckling or blossoming during coiling and uncoiling of deployable structures can be mitigated by applying a minimum value of tension force to the structure [13]. Previous boom deployment mechanisms have used a belt wrapped and deployed with the boom to apply this force on the boom [14].

Our deployment mechanism applies a uniform external pressure to the deployable structure by wrapping the structure between four thin 300 mm wide tensioned polyimide membranes. The membrane tensions are applied by connecting the membranes between four inner cylinders at one end and four stationary rollers at the other end. The four inner cylinders are arranged in a circular pattern and are rotated about a central vertical axis by an electric motor. Contacts between the cylinders and the deployable structure transfer the rotation of the motor to the structure, allowing active control of the coiling and uncoiling process through a central motor. The four stationary rollers are actuated by motors tensioning the polyimide films, according to the simple relation:

$$F = \frac{T}{R_r} \tag{1}$$

where F is the total tension on the membrane, T is the torque on the motor, and R_r is the radius of the rollers. This membrane tension is applied as pressure on the strips, and reacted by the four inner cylinders, as shown in Figure 7a. Independent closed-loop torque control on the roller motors provide constant tension on the films so that uncoiling synchronization of the strips is not required.

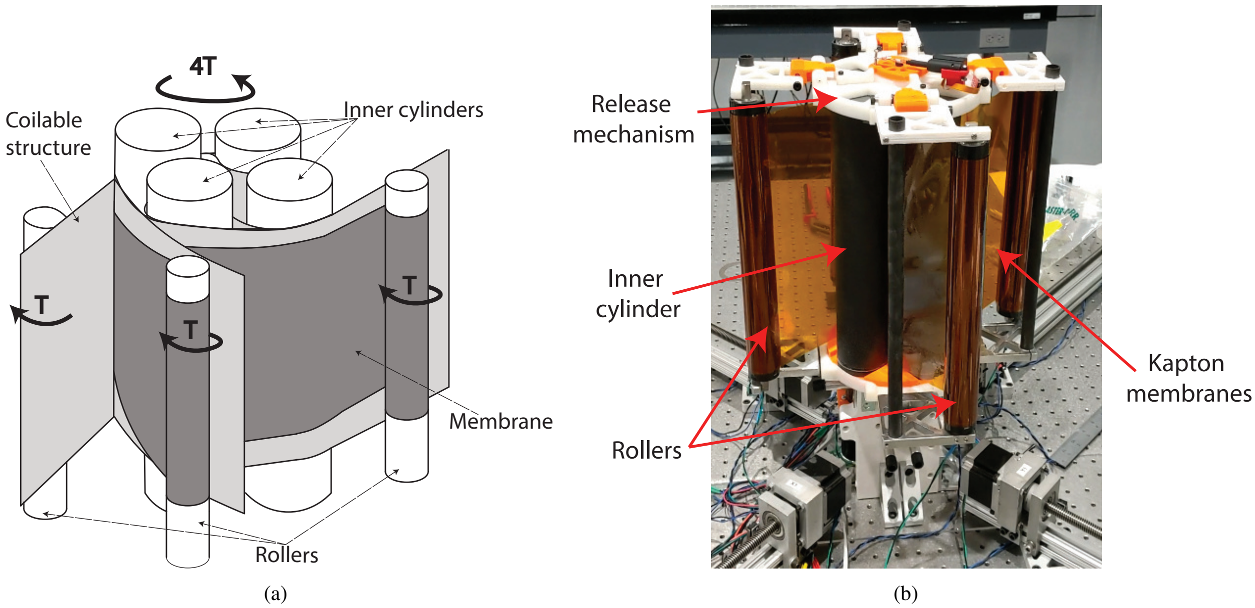

Fig. 7 (a) Concept of packaging and deployment mechanism using pressure; and (b) prototype of pressure stabilizing packaging and deployment mechanism.

At the end of the uncoiling, the coiling mechanism is deployed to allow the structure to unfold. First, the inner cylinders are extracted from the center of the mechanism by the tension of the films along designated grooves in top and bottom support plates. Then, a release mechanism synchronously deploys the four external rollers which rotate around spring-loaded hinges connecting them to a bottom support plate.

The radius of the inner cylinders is the maximum bending radius applied to the strips. Therefore, the minimum radius primarily depends on the maximum curvature that can be applied to the longerons and is independent of the size of the deployable structure coiled in it. Since individual longerons can be coiled without damage on cylinders as small as 25.4 mm in diameter, a safety factor of 2.5 was chosen on the coiling diameter, resulting in ⌀63.5 mm inner cylinders for the deployment mechanism. These four inner cylinders were arranged with a maximum diameter of 165 mm. The coiled diameter of the packaged structure is the sum of the diameter of the coiling mechanism the thickness of the coiled structure and the polyimide films wrapped around it. For the structural prototype used for this experiment, a coiled diameter of 185 mm was measured using a laser scanner.

The minimum height of the mechanism corresponds to the width of the flattened strips, which was 255 mm by design. To tolerate misalignments during coiling, 25 mm clearance was added on both sides of the longerons, resulting in 305 mm-long inner cylinders.

The tension applied to the polyimide film during coiling directly relates to the pressure applied to the strips. Its minimum value depends on the mechanical and geometric properties of the longerons. Preliminary tests had shown that uniform coiling of a strip is achieved when a tension of at least 10 N is applied to the membrane. However, the effects of the membrane tension on the stability and packaged dimension of the deployable structure have not been studied in detail yet and require further investigation. During the coiling experiments presented in this paper, the tension applied to the membranes was 25 N; the coiling mechanism is designed to provide up to 50 N tension.

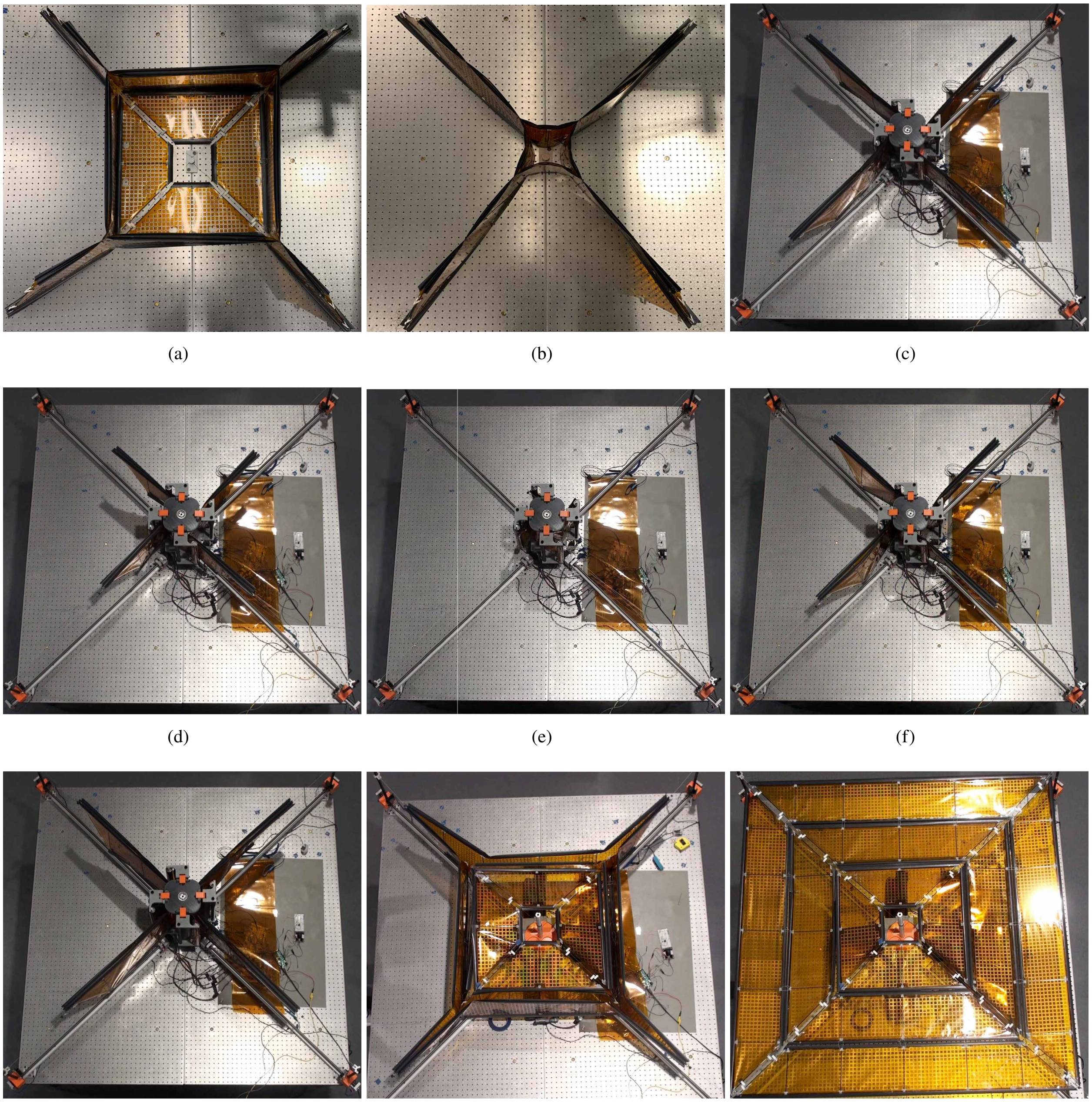

(a) (b) (c) (d) (e) (f) (g) (h) (i)

Fig. 8 The prototype (a) after the first step of folding on the optical table; (b) fully folded into the star shape on the optical table; (c) in the star shape inside the mechanism prior to coiling; (d) partially coiled inside the mechanism; (e) fully coiled inside the mechanism; (f) partially uncoiled; (g) after complete uncoiling and the first step of unfolding; (h) fully deployed.

B. Cord management system

The spherical terminals on one side of the cord were inserted into matching holes in the shaft and locked in place by a collar. The other side of the cords was attached to spring-loaded cord retractors capable of extending up to 800 mm and tensioned to less than 4 N.

A small pulley mounted on a carbon fiber rod allows adjusting the height of the cord and alignment with the cord location at the central shaft of the coiling mechanism. The carbon fiber rod is supported by a slider moving along the diagonal of the structure through a stepper motor-lead screw mechanism. In a flight implementation of the space structure these lead-screw mechanisms would be replaced by deployable booms.

C. Unfolding

During unfolding, the space structure deploys by releasing the elastic energy stored in the strips. The deployment scheme was designed sequentially remove constraints from the structure such that the unfolding would follow a predictable set of configurations. The number and location of the constraints was chosen based on an analytical model of the unfolding kinematics [15] and deployment tests on the structural prototype. Based on the model, a two-step release process allowing the structure to deploy along a kinematic path compatible with the boundary condition applied was chosen. To demonstrate the unfolding scheme, hairpins were used as constraints and the release was done manually, by removing four hairpins at a time. In future implementations, the hairpins will be replaced by remotely controlled automatic release devices.

IV. Prototype deployment

The mechanism described in Section III was used to demonstrate deployability of the prototype described here. The structure was folded in two steps, first resulting in the intermediate configuration shown in Figure 8a and finally in the star shape in Figure 8b. Hair pins were used to impose localized folds in the longerons at the desired locations based on analytical work and hold the structure in the folded configuration. The fold locations shown in Figure 4 were used as the nominal locations of the hairpins. The folded structure was placed into the mechanism and fully packaged as shown in Figure 8c. Subsequently, the mechanism was rotated to uncoil the structure (Figure 8d). Finally, the structure was unfolded in two steps: first, concurrently removing the four hair pins closest to the center of the structure resulting in the configuration shown in Figure 8e and subsequently removing the outer four hair pins, resulting in the fully deployed configuration (Figure 8f). This sequential unfolding scheme resulted in the staged dynamic deployment of the structure. By defining intermediate configurations for the structure, we provide a deterministic unfolding. The longerons and battens remained in pristine condition with no observable damage after multiple folding, packaging, and deployment iterations.

V. Mass and scaling to larger deployable structures

The 1.7 m $\times$ 1.7 m deployable space structure demonstrated here weighs 394 g and has an areal density of 136 g/m^2. Longerons account for most of the prototype's mass (42%) with the mass-representative polyimide weighing almost as much (41%). Table 1 lists the prototype's component mass breakdown and anticipated mass scaling to larger sizes. The mass of larger deployables is computed by generating a design for each of these deploaybles adjusting the lab prototype for cross-sectional and geometrical properties and generating the corresponding parts list.

The active area, i.e. the area of the mass-representative functional element surrogate in the prototype, is 2.22 m^2, 75.8% of the total area. The packaged diameter and height are 185 mm and 255 mm, respectively.

Table 1 Deployable space structure mass and scaling

Component	**1.7 m $\times$ 1.7 m (prototype)**	**25 m $\times$ 25 m**	**60 m $\times$ 60 m**
Longerons	166.9 g	12.5 kg	72.3 kg
Battens	31.2 g	6.7 kg	38.5 kg
Interfaces and adhesive	35.9 g	1.1 kg	3.6 kg
Functional material	160.1 g (50 μm thick polyimide)	58.9 kg (100 g/m^2)	340.1 kg (100 g/m^2)
Total	394.2 g (136 g/m^2)	79.2 kg (126.7 g/m^2)	454.5 kg (126.3 g/m^2)

VI. Conclusion

Packaging and deployment of an ultralight (136 g/m^2) structure made from thin shell longerons and battens integrated with a functional material surrogate film has been demonstrated for the first time. The structure was packaged in a cylinder with diameter of 185 mm and height of 255 mm inside a deployment mechanism and subsequently successfully deployed in lab. Design, manufacture, and integration of thin shells into a structure were critical elements of successfull development. The prototype design is based on a scalable concept and the components are designed for the bending stiffness of a 60 m × 60 m structure.

A mechanism to controllably package and deploy the structure was developed. The coiling and folding behavior of the thin-shell based deployable structure described here led to a mechanism packaging and deployment concept wherein pressure is applied to the structure by means of tensioning a membrane that wraps around the structure. This mechanism centrally controls the deployment through a set of motors and does not rely on booms to carry a tension load. It is designed to be scalable to structures up to 60 m × 60 m.

The successful lab deployment of the structure and demonstration of its deployment mechanism are key milestones toward the realization of ultralight and tightly packaged deployables in space. In the future, we aim to demonstrate deployment of this type of structure on-orbit, making possible a host of ambitious high-performance space missions.

Acknowledgments

Financial support from the Space Solar Power Project at Caltech is gratefully acknowledged.

References

[1] Glaser, P. E., "Power from the sun: Its future," *Science*, Vol. 162, No. 3856, 1968, pp. 857–861.

[2] Arya, M., Lee, N., and Pellegrino, S., "Ultralight structures for space solar power satellites," *3rd AIAA Spacecraft Structures Conference*, 2016, p. 1950.

[3] Royer, F., and Pellegrino, S., "Ultralight Ladder-type Coilable Space Structures," *AIAA SciTech Forum*, 2018.

[4] Kelzenberg, M. D., Espinet-Gonzalez, P., Vaidya, N., Roy, T. A., Warmann, E. C., Naqavi, A., Loke, S. P., Huang, J.-S., Vinogradova, T. G., Messer, A. J., Leclerc, C., Gdoutos, E. E., Royer, F., Hajimiri, A., Pellegrino, S., and Atwater, H. A., "Design and Prototyping Efforts for the Space Solar Power Initiative," *IEEE PVSC*, 2017.

[5] Gdoutos, E. E., Leclerc, C., Royer, F., Kelzenberg, M. D., Warmann, C., Emily, Espinet-Gonzalez, P., Vaidya, N., Bohn, F., Abiri, B., Hashemi, M. R., Gal-Katziri, M., Fikes, A., Atwater, H. A., Hajimiri, A., and Pellegrino, S., "A lightweight tile structure integrating photovoltaic conversion and RF power transfer for space solar power applications," *AIAA SciTech Forum*, 2018.

[6] Hashemi, M. R. M., Fikes, A. C., Gal-Katziri, M., Abiri, B., Bohn, F., Safaripour, A., Kelzenberg, M. D., Warmann, E. L., Espinet, P., Vaidya, N., Gdoutos, E. E., Leclerc, C., Royer, F., Pellegrino, S., Atwater, H. A., and Hajimiri, A., "A flexible phased array system with low areal mass density," *Nature Electronics*, Vol. 2, No. 5, 2019, pp. 195–205. doi:10.1038/s41928-019-0247-9, URL `https://doi.org/10.1038/s41928-019-0247-9`.

[7] Gdoutos, E., Leclerc, C., Royer, F., Türk, D. A., and Pellegrino, S., "Ultralight Spacecraft Structure Prototype," *AIAA SciTech Forum*, 2019. doi:10.2514/6.2019-1749, URL `https://arc.aiaa.org/doi/abs/10.2514/6.2019-1749`.

[8] Murphey, T. W., and Banik, J., "Triangular rollable and collapsible boom," , Mar. 1 2011. US Patent 7,895,795.

[9] Leclerc, C., Wilson, L. L., Bessa, M. A., and Pellegrino, S., "Characterization of ultra-thin composite triangular rollable and collapsible booms," *4th AIAA Spacecraft Structures Conference*, 2017, p. 0172.

[10] Leclerc, C., and Pellegrino, S., "Reducing Stress Concentration in the Transition Region of Coilable Ultra-Thin-Shell Booms," *AIAA SciTech Forum*, 2019. doi:10.2514/6.2019-1522, URL `https://arc.aiaa.org/doi/abs/10.2514/6.2019-1522`.

[11] Royer, F., and Pellegrino, S., "Buckling of Ultralight Ladder-type Coilable Space Structures," *AIAA SciTech Forum*, 2020.

[12] Türk, D. A., and Pellegrino, S., *Parametric Design of Conforming Joints for Thin-Shell Coilable Structures*, ???? doi: 10.2514/6.2019-1259, URL `https://arc.aiaa.org/doi/abs/10.2514/6.2019-1259`.

[13] Wilson, L., Gdoutos, E. E., and Pellegrino, S., "Tension-Stabilized Coiling of Isotropic Tape Springs," *International Journal of Solids and Structures*, 2019. doi:https://doi.org/10.1016/j.ijsolstr.2019.09.010, URL `http://www.sciencedirect.com/science/article/pii/S0020768319304226`.

[14] Sproewitz, T., Grundmann, J. T., Seefeldt, P., Spietz, P., Hillebrandt, M., Jahnke, R., Mikulz, E., Renger, T., Reershemius, S., Sasaki, K., Sznajder, M., and Tóth, N., "Membrane Deployment Technology Development at DLR for Solar Sails and Large-Scale Photovoltaics," *2019 IEEE Aerospace Conference*, 2019, pp. 1–20. doi:10.1109/AERO.2019.8741630.

[15] Pedivellano, A., Gdoutos, E. E., and Pellegrino, S., "Sequentially controlled dynamic deployment of ultra-thin shell structures," *AIAA SciTech Forum*, 2020.